COMPARABILITY OF NON-DESTRUCTIVE MOISTURE MEASUREMENT TECHNIQUES ON MASONRY DURING SIMULATED WETTING

S.A. Orr[1], H.A. Viles[1*], A.B. Leslie[2] and D. Stelfox[3]

Abstract

Detecting the presence of moisture in historical masonry is essential to understanding how a structure interacts with the environment, and diagnosing the potential for damage from a range of physical, chemical, and biological processes. In-situ, non-invasive diagnostic techniques have been developed in preference to methods that require irreversible modifications to a structure. These techniques include: electrical resistivity, microwaves, and infrared thermography. Independently, these approaches provide limited snapshots of surficial and internal moisture regimes; this project sought to assess the comparability of multiple techniques. Simulated post-rain spell drying was monitored over 48 h on limestone and sandstone monoliths in a controlled laboratory environment and also in ambient conditions on purpose-built masonry located in Oxfordshire, UK. Repeat measurements were taken using electrical resistance tomography (ERT), electrical and microwave moisture meters, and infrared thermography. Three aspects of comparability are discussed: i) data transformations and geological comparability, ii) depth-resolving meter readings, iii) the localised benefits of employing multiple technologies and instruments.

Keywords: moisture mapping, drying processes, non-destructive testing (NDT), instrument comparability, stone masonry

1. Introduction

Water is an important factor in stone deterioration, acting as a primary and secondary agent in a range of chemical, physical, and biological deterioration mechanisms. The role of water in specific mechanisms depends on its spatial and temporal patterning (Mamillan 1981). To this end, it is necessary to be able to detect and monitor local variation of water within stonework and masonry structures.

Non-invasive moisture monitoring techniques have been developed for the historical environment as an alternative to invasive techniques. These include electrical resistance tomography (ERT), which has been employed to successfully monitor short-term moisture

[1] S.A. Orr and H.A. Viles*
School of Geography and the Environment, University of Oxford, United Kingdom
heather.viles@ouce.ox.ac.uk

[2] A.B. Leslie
Historic Environment Scotland, United Kingdom

[3] D. Stelfox
Consarc Design Group, United Kingdom

*corresponding author

regimes in historic masonry (Martinho *et al*. 2010). In contrast, thermography and handheld moisture meters (or 'damp' meters) have been adopted from civil engineering, but are primarily intended for use on twentieth-century materials. Handheld meters have been assessed for relative performance and best practice (Eklund *et al*. 2013) for use on stone but their applicability to masonry with regards to how they compare to more robust analytical equipment is yet to be established. This paper compares two handheld moisture meters and infrared thermography to electrical resistance tomography to investigate moisture dynamics, discussing aspects of technological comparability for complex masonry constructions and information gained by combining multiple devices.

2. Materials and methods

2.1. Materials

Two stone monoliths were used – a sandstone block measuring 55×32×25.5 cm (obtained from a quarry) and a limestone block (from a waste site) measuring 71×38 cm in height and length respectively (see Fig. 1a), with an uneven width varying from 9–20 cm. The limestone block has a discoloration running down the front surface suggesting near-surface physical inconsistencies, and could be indicative of defects at further depths.

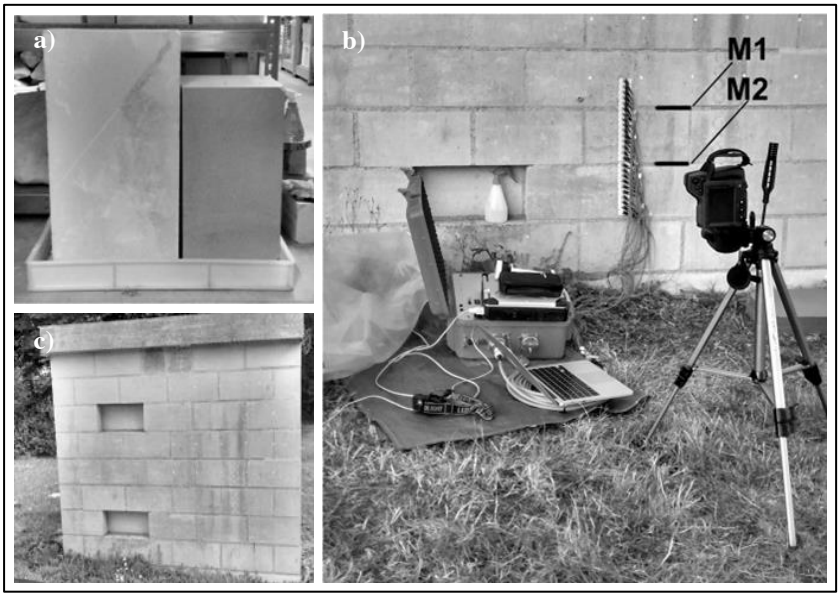

Fig. 1: The monoliths (left, limestone; right, sandstone) (a) and the traditional masonry construction (b). An example of the simultaneous instrument set-up with positions of the mortar joints: M1 and M2 (c).

The masonry construction is 1.8 m high and 2.0 m wide, and comprises a single skin of Elm Park limestone ashlar blocks (20×20×40 cm) with 2 cm lime mortar joints (Fig. 1b). It is located in a field with sparse tree cover in Oxfordshire, England. Measurements were taken in July 2015. The wall has an exposed western façade that receives direct sunlight between 13:00–15:00 h and 17:00–19:00 h daily in summer if not obscured by cloud cover.

2.2. Experimental protocol

This study monitored drying for 48 h after simulated rain events across 48 cm vertical transects of 25 evenly-spaced 2 cm nodes. The ERT apparatus could not be removed from the stone surface for the employed time scales, so handheld meter measurements were taken on a parallel transect separated from the former by 8 cm (Fig. 1c). Preliminary testing on the monoliths demonstrated two ERT transects separated by 15 cm and equally-distanced from the edges were highly correlated, and had similar wetting and drying properties (Orr 2015). Thus, the parallel transects were considered to be comparable representations of drying processes, with error $\leq$ 15%. The monoliths were equilibrated and tested under stable temperature and *RH*.

Moisture instrument readings were taken along the transects at hourly intervals for the initial 12 h of drying, after which measurements were taken at 3, 6, 12 and 24 h; this timescale captures the dynamic nature of surface desorption through evaporation. For unsaturated flow in porous media the cumulative moisture migration i (in this case, i_{drying}) can be defined as $i_{dry} = Rt^{1/2}$,in which R is a material property of desorptivity equal to the Boltzman transformation $\varphi = xt^{1/2}$ integrated over a moisture content θ differential for a vertical distance x in time t (Hall and Hoff 2012, p. 114). This relationship dictates that rates of desorption decrease significantly with time; deviations typically occur in fabricated materials and were unexpected for the selected stones (Hall and Hoff, 2012, p. 129).

A driving rain index was derived to determine the quantity of water that should be applied to emulate driving rain spells based on EN ISO 15927-3:2009 for the Oxfordshire field site. Meteorological data was taken from the UK MIDAS database at a site ~20 km from the site; in predominantly flat regions, indices are applicable up to 100 km away. The following parameters were employed:

- Roughness factor for Tier II terrain for 'farm land with boundary hedges, occasional small farm structures, houses or trees'
- Wall geometry factor = 0.4, reflecting the lower portion of a 'two-story building with flat roof (pitch < 20°)'
- Topography and obstruction factors = 1, i.e. no index reductions

The determined spell index I_S is the 67th percentile of I'_S, representing the maximum value of I'_S likely to occur in a three year period. A wall spell index = 6.5 $L \cdot m^{-2} \cdot h^{-1}$ (calculated for 1985–2014) of distilled water was applied over 1 h with a small pressured spray bottle in roughly rectangular areas surrounding the transects.

2.3. Instrumentation

A GeoTom device (Geolog2000; Augsburg, Germany) was used to collect the two-dimensional resistance profiles in conjunction with crocodile clip shielded cables and self-adhesive electrocardiogram electrodes affixed to the stone surface. Adhesive electrodes were used instead of drilled-in steel electrodes as they are non-invasive, and have been shown to have similar contact resistance to implanted steel electrodes (Sass and Viles 2006). Data were collected with a linear Wenner array and inverted into apparent resistivity models using RES2DINV v. 3.59 (GeoTomo Software; Malaysia).

Electrical resistance is also influenced by material properties, physical characteristics, and salts (Martinho *et al*. 2010) which creates ambiguity leading to misinterpretation of direct-current measurements (Kruschwitz 2007, p. 2). However, ERT has been shown to relate to

moisture contents with gravimetric calibration methods (Sass 1998) through an extension of Archie's Law relating saturation and resistivity with the appropriate assumptions (Sass and Viles 2010). Lime mortar has been shown to have commensurate dielectric properties to limestone (Ball *et al*. 2011). In addition to ERT, the following were used to monitor moisture:

- Surveymaster Protimeter (GE Measurement & Control; Billerica, MA, USA) includes a pin-type resistance meter with a sensor consisting of two 10 mm long stainless steel pins spaced approximately 14 mm apart, a wood moisture equivalent (WME) from 0–100.
- T610 (Trotec; Marchtrenk, Austria) produces a microwave field penetrating 20-30 cm that is subsequently reflected and converted into nominal values from 0-200.
- T460 thermal imaging camera (FLIR; Wilsonville, OR, USA) was used to capture surface temperatures of the monoliths and masonry wall areas surrounding the transects; it has a thermal sensitivity of <0.03°C and an output resolution of 240×320 pixels.

3. Results and discussion

3.1. Data transformations

ERT timeseries were logarithmically transformed and normalised to initial, pre-wetting stage resistivities (ρ_{pw}). These do not represent completely 'dry' states; the pre-wetting measurements represent the stone at a particular phase of hygrothermal transition. The transformed resistivities $\rho'_i = -log_{10}(\rho_i/\rho_{pw})$ enabled comparison between the monoliths and the masonry construction at depths with pseudo-values linearly proportional to moisture contents. Values of ρ'_i theoretically range within (∞, 0); as $\rho' \rightarrow 0$ the resistivity (and thus purported moisture content) are returned to the pre-wetting stage. Practically, values of ρ' did not exceed 2.

Inversion uncertainties were greater for the pre-wetting states, tending to increase over the duration of the drying process: this is likely caused by the software's difficulty with handling the geological realism of inverting very dry stone (Sass and Viles 2010). This complicated obtaining appropriate values of ρ_{pw}; however, the benefit of lognormal transformation is that the pre-wetting denominator induces only a vertical shift of ρ' in the lognormal dimension. While pre-wetting resistivities can be analysed, two parameters independent of this enable valuable discussion: i) the shape of the drying curve, and ii) $\Delta\rho_{f-0}$.

The meter readings ν exhibit linear behaviour similar to the ERT depth ρ' curves (Fig. 2). This suggests that the instrument readings calibrate linearly to moisture contents. This implies that relative meter readings (additive/subtractive from a reference value, i.e. $\Delta\nu_{ref-i}$) can be considered proportional to moisture contents. While the idea of 'relative readings' is not novel in moisture meter best practice, previous guidance has suggested using ν_i/ν_{ref} (Burkinshaw and Parrett 2003); this relationship is not ideal for interpreting the readings of some handheld meters.

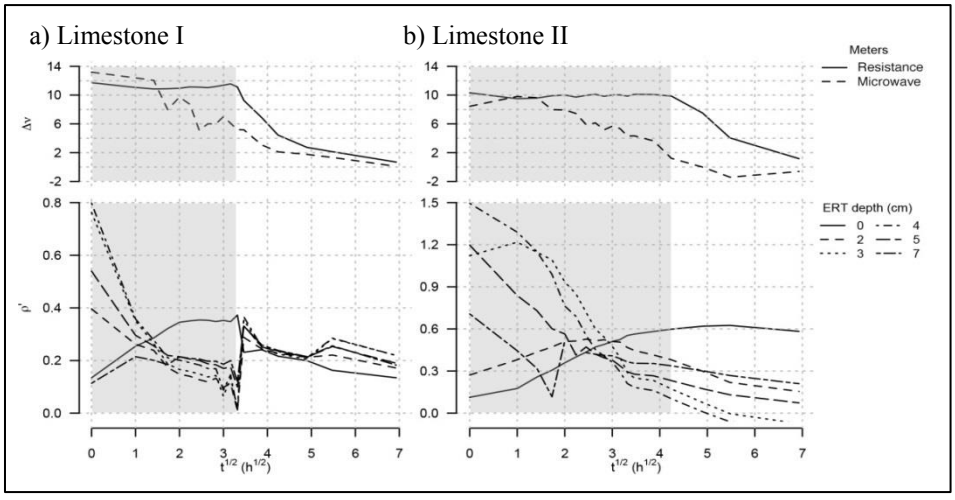

Fig. 2: Transformed meter readings Δν and ERT depth moisture profiles ρ′ for two iterations of the limestone monolith moisture regimes.

The surface resistance meter captured a constant surface value of moisture before decreasing to the pre-wetting conditions, which corresponds to the inversion of the ERT surface measurement. It has been shown that this meter model is able to produce WMEs higher than these values on English limestones (Eklund *et al*. 2013), so it was not suspected to represent moisture contents out of instrumental range.

3.2. Depth-resolved damp meter modelling

No single ERT depth profile was found to characterise the moisture meter readings over the total drying duration in isolation: there were periods when certain depths had Pearson's $R > 0.8$, but negative coefficients indicated relationships to a lack of moisture following a migration to adjacent depth(s). To this end, multiple linear regression models were created using non-negative least squares (NNLS) regression for each of the monolith and stone masonry experimental runs.

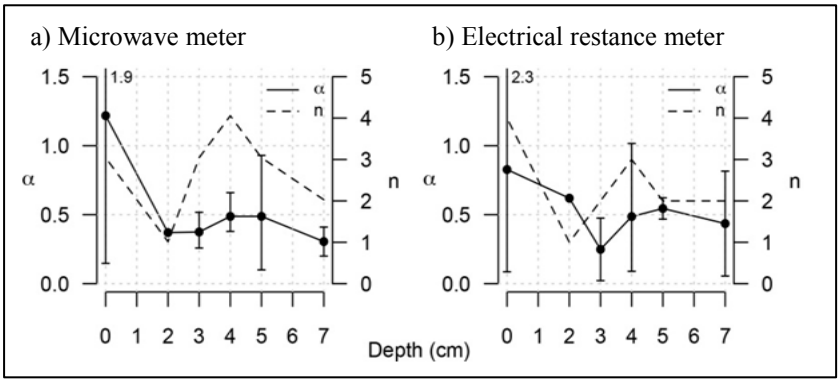

Fig. 3: NNLS regression results for handheld meters: Coefficients α and quantity of regression models incorporating depth. Vertical bars indicate maxima and minima.

NNLS is a least squares regression in which coefficients are restricted to positive values, based on an algorithm developed by Lawson and Hanson (1995). As the residuals of a NNLS regression are not normally distributed, typical evaluation parameters (eg. confidence intervals, p-values) are not applicable, so each predictor column (ERT depths) and the meter reading vectors were normalised between 0 and 1 (Slawski *et al*. 2013): regressions coefficients represent the relative contributions of independent variables. Both handheld meters exhibited decreasing correlation with the ERT as depth increased, an effect that was seen more strongly with the microwave meter (Fig. 3).

3.3. Multi-instrument utility

The surface resistance meter captured distinct mortar behaviour due to the high resolution and localised readings. In contrast, the microwave meter and ERT did not capture distinct moisture movements through the mortar as clearly due to wider detection range and smoothing techniques, respectively.

Passive IR thermography was able to capture early rapid edge-adjacent evaporation transitioning to front surface evaporation in the stone monoliths, in addition to subsequent higher moisture concentrating at the base, adjacent to an impermeable plastic barrier (Fig. 4). These phenomena are difficult to assess or characterise with other non-destructive techniques due to interference from the adjacent air space.

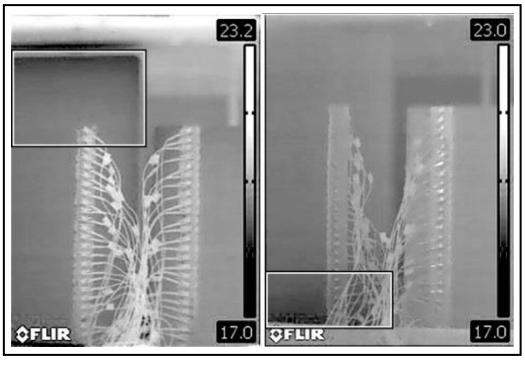

Fig. 4: A distinct transfer of significant moisture migration at monolith edges mid-drying (left) and collected base water at 48 h (right) is highlighted in boxes, where darker zones represent areas of higher moisture content.

Mortar-adjacent behaviour was assessed by comparing the mortar moisture contents to the adjacent ashlar units: positive values represent mortar readings greater than the surrounding areas, as would be expected for a more porous building material designed to aid moisture migration through masonry.

The early electrical mortar readings were commensurate to the surrounding stone representing similar moisture contents during the latent phase of activity, after which mortar moisture contents increase (Fig. 5). Differences in dielectric properties can be discounted as a crucial factor: pre-wetting readings differed by 0.1 WME between the mortar joints and the surrounding stonework, respectively. The microwave meter captures the mortar joint behaviour to a lesser extent: there is significant variation above and below the mortar joint during the latent phase of moisture transport but mortar meter readings are

similar to the electrical resistance meter after $t^{1/2} = 2$. In contrast, ERT does not exhibit any distinct near-mortar behaviour.

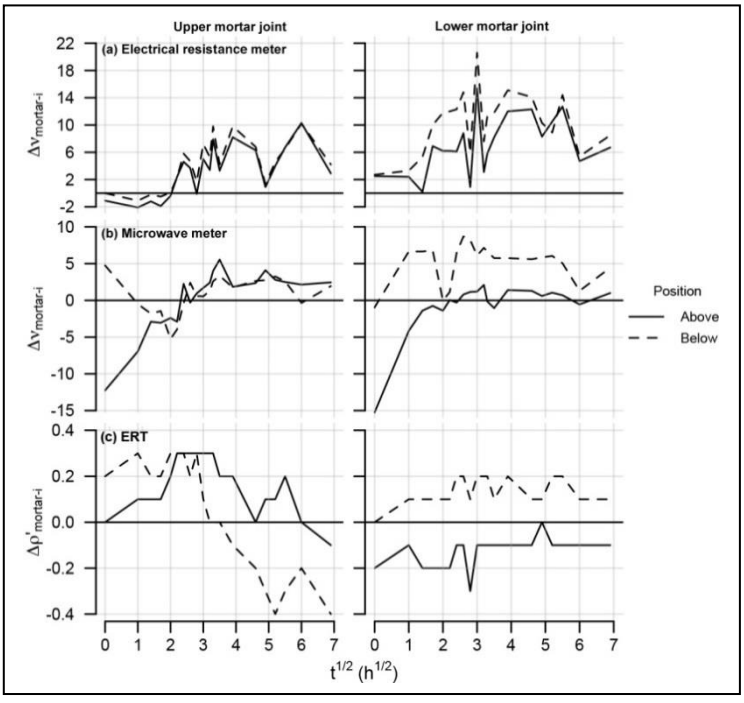

Fig. 5: Differential instrument readings above and below mortar joints within the stone for the electrical resistance meter (a), the microwave meter (b), and ERT (c). Values are presented relative to the upper (M1) and lower (M2) mortar joint values (see Fig. 1c); positive values represent higher moisture than the surrounding areas.

4. Conclusions

Spatial and temporal comparisons of data from handheld moisture meters and infrared thermography with electrical resistance tomography produced valuable information on how instrument measurements interacted with the masonry elements. Distinct mortar joint and near-edge behaviour was distinguished by the handheld meters and infrared thermography, identifying important characteristics of moisture migration that would have otherwise been unnoticed by ERT. Although handheld meter signals may penetrate a certain range, they are less attuned to detecting water at greater depths as their readings are more representative of near-surface moisture regimes. Identifying building elements and conditions for which instrument types are most applicable enables efficient moisture surveys, but interpretation should consider different building materials and, if possible, incorporate laboratory validation.

Acknowledgements

Many thanks to Hong Zhang and Mona Edwards for logistical support. This work was enabled by financial support provided by the EPSRC through the Centre for Doctoral Training in Science and Engineering for Arts, Heritage, and Archaeology.

References

Ball, R. J., Allen, G. C., Starrs, G., and McCarter, W. J., 2011, Impedance spectroscopy measurements to study physio-chemical processes in lime-based composites, Applied Physics A, 105(3), 739–751.

EN ISO 15927-3:2009 –Hygrothermal performance of buildings. Calculation and presentation of climatic data. Calculation of a driving rain index for vertical surfaces from hourly wind and rain data.

Burkinshaw, R. and Parrett, M., 2003, Diagnosing Damp. RICS Books, London, UK.

Eklund, J.A., Zhang, H., Viles, H.A., and Curteis, T., 2013, Using handheld moisture meters on limestone: Factors affecting performance and guidelines for best practice, International Journal of Architectural Heritage, 7(2), 207–224.

Hall, C. and Hoff, W.D., 2012, Water Transport in Brick, Stone and Concrete, 2nd ed., Taylor & Francis Group, London, UK.

Kruschwitz, S.F., 2007, Assessment of the Complex Resistivity Behaviour of Salt Affected Building Materials, Ph.D. thesis, Technischen Universitaet Berlin, Germany.

Lawson, C.L. and Hanson, R.J., 1995, Solving Least Squares Problems, Society for Industrial and Applied Mathematics, Philadelphia, USA.

Mamillan, M., 1981, Alteration et Durabilité des Pierres. In proceedings of Seminaire Alteration et Durabilité des Bétons et des Pierres, St.Remy-Les-Chevreuse, France.

Martinho, E., Alegria, F., Grangeia, C., Dionisio, A., and Almeida, F., 2010, Electrical resistivity imaging: Overview and a case study in stone cultural heritage. In: 3D Imaging: Theory, Technology, and Applications, Duke, E.H. and Aguirre, S.R (eds.).

Orr, S.A., 2015, Comparative synthesis of handheld damp meters and infrared thermography with 2D-resistive tomography, M.Res. thesis, UCL.

Sass, O. and Viles, H.A., 2006, How wet are these walls? Testing a novel technique for measuring moisture in ruined walls, Journal of Cultural Heritage, 7(4), 257–263.

Sass, O. and Viles, H.A., 2010, Wetting and drying of masonry walls: 2D-resistivity monitoring of driving rain experiments on historic stonework in Oxford, UK, Journal of Applied Geophysics, 70(1), 72–83.

Slawski, M., Hein, M., 2013, Non-negative least squares for high-dimensional linear models: Consistency and sparse recovery without regularization, Electronic Journal of Statistics, 7, 3004–3056.